Nonlinear Single-Particle Dynamics in High Energy Accelerators

Part 1: Introduction

Examples of nonlinear dynamics in accelerator systems

Nonlinear Single-Particle Dynamics in High Energy Accelerators

This course consists of eight lectures:

1. Introduction – some examples of nonlinear dynamics

2. Basic mathematical tools and concepts

3. Representations of dynamical maps

4. Integrators I

5. Integrators II

6. Phase space portraits and "phenomenology"

7. Normal form analysis

8. Some numerical techniques

Objectives of the Course

By the end of the course, you should be able to:

- perform simple dynamical calculations using action-angle variables;

- evaluate a Lie transformation as a Taylor series (up to some order);

- use generating functions to express nonlinear maps in implicit form;

- apply integrator methods to express nonlinear maps in explicit form;

- describe nonlinear phenomena in terms of features in phase space portraits;

- perform normal-form analysis of linear and nonlinear maps;

- describe the use of numerical techniques such as frequency maps analysis, to analyse the characteristics on complex nonlinear systems.

References

H. Goldstein, "Classical Mechanics," Addison-Wesley (2nd edition, 1980).
A classic text on classical mechanics. The chapters on the Hamilton Equations of Motion and Canonical Transformations are especially relevant. A new edition is also available.

E. Forest, "Beam Dynamics: A New Attitude and Framework," Taylor and Francis (1998).
A treasure-trove, though somewhat daunting. Highly relevant.

A.J. Dragt, "Lie Methods for Nonlinear Dynamics with Applications to Accelerator Physics," (2009).
http://www.physics.umd.edu/dsat/dsatliemethods.html
Encyclopaedic. Highly recommended.

References

A.W. Chao and M. Tigner (editors), "Handbook of Accelerator Physics and Engineering," World Scientific (1999).
Section 2.3 (various authors) covers nonlinear dynamics.

L.E. Reichl, "A Modern Course in Statistical Physics," (1984).
Does not metion accelerators explicitly − but the section on ergodicity contains a very relevant example, and shows how widely some of the concepts of nonlinear dynamics occur in physics.

Introduction − some examples of nonlinear dynamics

In this lecture, we discuss some examples of nonlinear single-particle dynamics in common accelerator systems.

We shall consider:

1. longitudinal dynamics in a bunch compressor;

2. transverse dynamics in a (periodic) storage ring;

3. transverse dynamics in a final focus system.

By the end of the lecture, you should be able to describe the source of nonlinearities in the above systems, their effects, and the limitations that they impose.

Example 1: Bunch compressor

As a first example, we discuss nonlinear longitudinal dynamics in a bunch compressor. A bunch compressor is a system that reduces the length of a bunch, by performing a rotation in longitudinal phase space. Such systems are used, for example, in free electron lasers, to increase the peak current in a bunch.

We shall work through this example in some detail, almost as a case study, following these steps:

1. Outline of structure and operation of a bunch compressor.

2. Specification of parameters based on linear dynamics.

3. Analysis of linear and nonlinear effects.

4. Modification of parameters to compensate nonlinear effects.

Bunch compressor: structure and operation

Distribution of particles 'rotates' in longitudinal phase space (area is conserved).
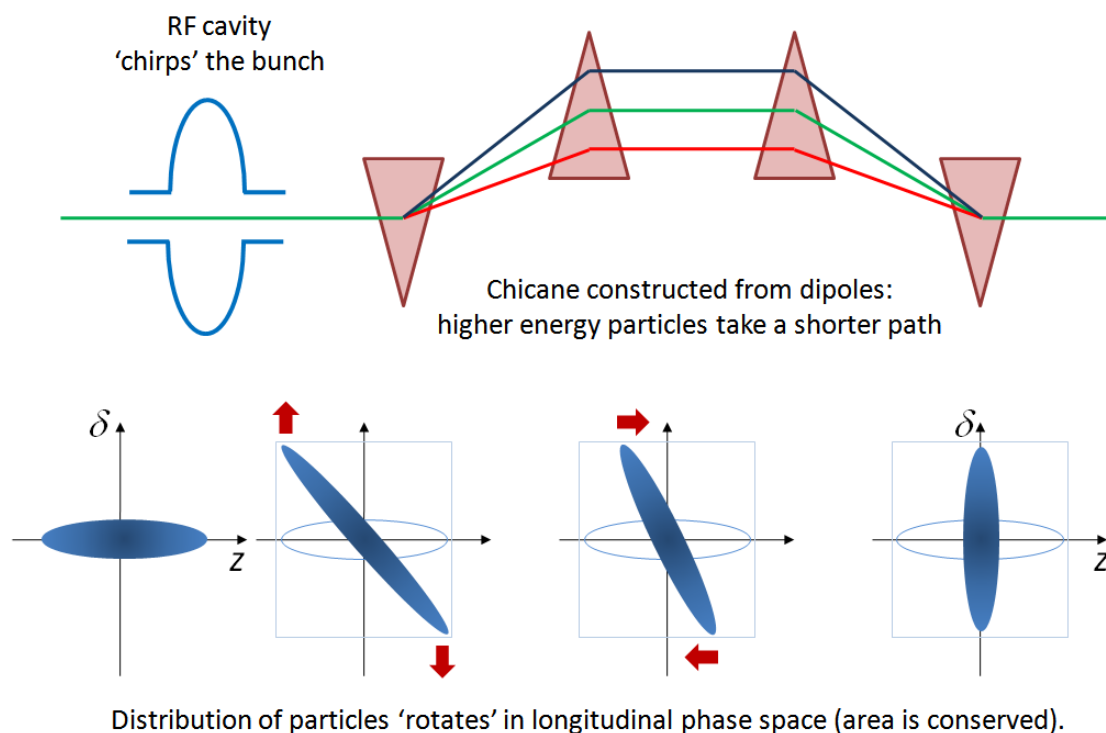
The rf cavity is designed to "chirp" the bunch, i.e. to provide a change in energy deviation as a function of longitudinal position within the bunch. We define the energy deviation δ as the energy error of a particle, with respect to a specified reference energy, E_0:

$$\delta = \frac{E - E_0}{\beta_0 E_0}. \tag{1}$$

The other longitudinal variable, z, is the distance that a particle is ahead of a nominal reference particle. With the simplifying approximation $\beta_0 \approx 1$, the dynamical map for the rf cavity in the bunch compressor is:

$$
\begin{aligned}
z &\mapsto z, & (2)\\
\delta &\mapsto \delta - \frac{eV}{E_0}\sin\frac{\omega z}{c}, & (3)
\end{aligned}
$$

where V is the rf voltage, and ω is 2π times the rf frequency.

The chicane does not change the energy of the particles (neglecting synchrotron radiation). However, the path length L depends on the energy of the particle.
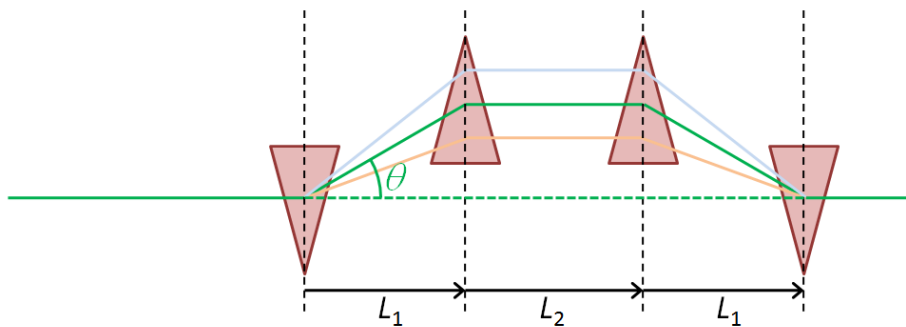
If we assume that the bending angle in a dipole is small, $\theta \ll 1$:

$$L = \frac{2L_1}{\cos\theta} + L_2 \tag{4}$$

The bending angle is a function of the particle's energy:

$$\theta = \frac{\theta_0}{1 + \delta}. \tag{5}$$

The complete map for the bunch compressor can be written as a map for the rf cavity (2), (3):

$$
\begin{aligned}
z &\mapsto z, \\
\delta &\mapsto \delta - \frac{eV}{E_0} \sin \frac{\omega z}{c},
\end{aligned}
$$

followed by a map for the chicane:

$$
\begin{aligned}
z &\mapsto z + 2L_1 \left(\frac{1}{\cos \theta_0} - \frac{1}{\cos \theta} \right), & (6) \\
\delta &\mapsto \delta, & (7)
\end{aligned}
$$

where θ_0 is the nominal bending angle of each dipole in the chicane, and θ is given by (5):

$$
\theta = \frac{\theta_0}{1 + \delta}.
$$

Clearly, the map is nonlinear. The question is: how important are the nonlinear terms?

Bunch compressor: linear dynamics

To understand the effect of the nonlinear part of the map, we shall look at a specific example. First, we will "design" a bunch compressor using only the linear part of the map, i.e. by completely ignoring the nonlinear terms. Then, we shall see how our design has to be modified to take account of the nonlinearities.

To first order in the dynamical variables z and δ, the map for the bunch compressor can be written:

$$
\begin{aligned}
z &\mapsto z, & (8) \\
\delta &\mapsto \delta - \frac{eV}{E_0} \frac{\omega z}{c}, & (9)
\end{aligned}
$$

followed by:

$$
\begin{aligned}
z &\mapsto z + 2L_1 \frac{\theta_0 \sin \theta_0}{\cos^2 \theta_0} \delta. & (10) \\
\delta &\mapsto \delta. & (11)
\end{aligned}
$$

In a linear approximation, the maps for the rf cavity and the chicane may be represented as matrices:

$$M_{\mathsf{rf}} = \begin{pmatrix} 1 & 0 \\ -a & 1 \end{pmatrix}, \qquad M_{\mathsf{ch}} = \begin{pmatrix} 1 & b \\ 0 & 1 \end{pmatrix}, \qquad (12)$$

where:

$$a = \frac{eV}{E_0}\frac{\omega}{c}, \quad \text{and} \quad b = 2L_1\frac{\theta_0 \sin\theta_0}{\cos^2\theta_0}. \qquad (13)$$

The matrix representing the total map for the bunch compressor, M_{bc}, is then:

$$M_{\mathsf{bc}} = M_{\mathsf{ch}} \cdot M_{\mathsf{rf}} = \begin{pmatrix} 1-ab & b \\ -a & 1 \end{pmatrix}. \qquad (14)$$

The action of the map is written:

$$\begin{pmatrix} z \\ \delta \end{pmatrix} \mapsto M_{\mathsf{bc}} \cdot \begin{pmatrix} z \\ \delta \end{pmatrix}. \qquad (15)$$

We note in passing that the linear part of the map is *symplectic*. A linear map is symplectic if the matrix M representing the map is symplectic, i.e. satisfies:

$$M^{\mathsf{T}} \cdot S \cdot M = S, \qquad (16)$$

where, in one degree of freedom (i.e. two dynamical variables), S is the matrix:

$$S = \begin{pmatrix} 0 & 1 \\ -1 & 0 \end{pmatrix}. \qquad (17)$$

In more degrees of freedom, S is constructed by repeating the 2×2 matrix above on the block diagonal, as often as necessary. In one degree of freedom, it is a necessary and sufficient condition for a matrix to be symplectic, that it has unit determinant: but this condition does *not* generalise to more degrees of freedom.

We shall consider what it means to say that a nonlinear map is symplectic later in this course.

Now we proceed to derive expressions for the required values of the parameters a and b, in terms of the desired initial and final bunch length and energy spread.

We construct the beam distribution *sigma* matrix by taking the outer product of the phase space vector for each particle, then averaging over all particles in the bunch:

$$\Sigma = \langle \vec{z}\,\vec{z}^{\mathsf{T}} \rangle = \begin{pmatrix} \langle z^2 \rangle & \langle z\delta \rangle \\ \langle z\delta \rangle & \langle \delta^2 \rangle \end{pmatrix}. \tag{18}$$

The transformation of Σ under a linear map represented by a matrix M is given by:

$$\Sigma \mapsto M \cdot \Sigma \cdot M^{\mathsf{T}}. \tag{19}$$

Usually, a bunch compressor is designed so that the correlation $\langle z\delta \rangle = 0$ at the start and end of the compressor. In that case, using (14) for the linear map M, and (19) for the transformation of the sigma matrix, we find that the parameters a and b must satisfy:

$$(1 - ab)\frac{a}{b} = \frac{\langle \delta^2 \rangle_i}{\langle z^2 \rangle_i} \tag{20}$$

where the subscript i indicates that the average is taken over the *initial* values of the dynamical variables.

Given the constraint (20), the compression factor r is given by:

$$r^2 \equiv \frac{\langle z^2 \rangle_f}{\langle z^2 \rangle_i} = 1 - ab, \tag{21}$$

where the subscript f indicates that the average is taken over the final values of the dynamical variables.

As a specific example, consider a bunch compressor for the International Linear Collider:

Initial rms bunch length	$\sqrt{\langle z^2 \rangle_i}$	6 mm
Initial rms energy spread	$\sqrt{\langle \delta^2 \rangle_i}$	0.15%
Final rms bunch length	$\sqrt{\langle z^2 \rangle_f}$	0.3 mm

Solving equations (20) and (21) with the above values for rms bunch lengths and energy spread, we find:

$$a = 4.9937\,\mathrm{m}^{-1}, \quad \text{and} \quad b = 0.19975\,\mathrm{m}. \tag{22}$$

We can illustrate the effect of the linearised bunch compressor map on phase space using a "window frame" distribution:
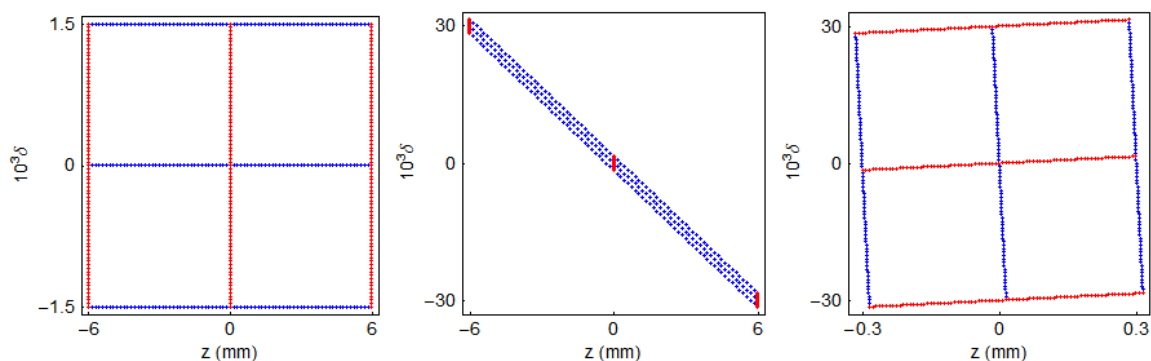
As expected, the bunch compressor rotates the distribution in phase space by (nearly) 90°. At the same time, the rms bunch length is reduced by a factor of 20. Note that the rms energy spread is *increased* by the same factor: because the map is symplectic, phase space areas are conserved under the transformation. Also note that, because the map is linear, straight lines in phase space remain straight.

Now let us see what happens when we apply the full nonlinear map for the bunch compressor to the full nonlinear distribution. The full map cannot simply be represented by the two parameters a and b: we need to make some assumptions for the rf voltage and frequency, and the dipole bending angle and chicane length. We have to choose these parameters so that the "linear" parameters have the appropriate values, but fortunately, this is not difficult.

Beam (reference) energy	E_0	5 GeV
RF frequency	f_{rf}	1.3 GHz
RF voltage	V_{rf}	916 MV
Dipole bending angle	θ_0	3°
Dipole spacing	L_1	36.3 m

It appears that we need a lot of rf voltage; it is still feasible (if expensive). Let us see what happens to the dynamics when we use these parameters...

As before, we illustrate the effect of the bunch compressor map on phase space using a "window frame" distribution:
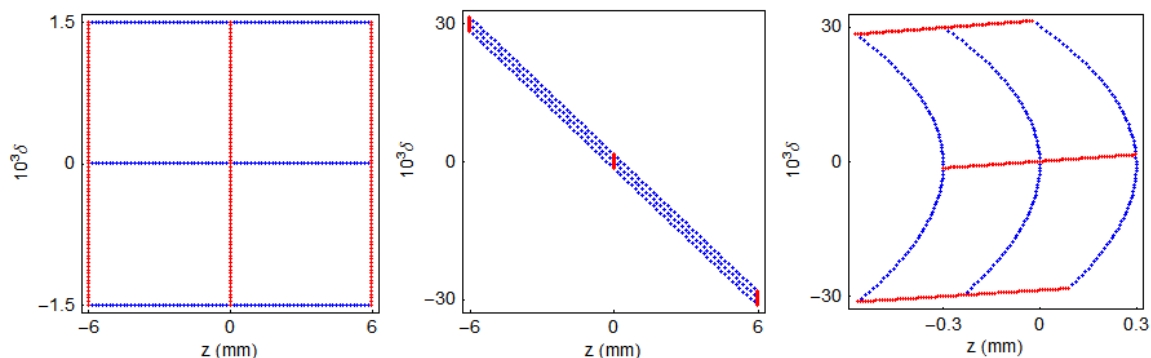
This looks bad. The map has had approximately the effect we desire: the bunch length has been reduced (and the distribution rotated by approximately 90°). However, there is significant distortion of the distribution. Because of the nonlinear terms in the map, straight lines do not stay straight. The rms bunch length will be significantly longer than we are aiming for.

Whether or not the nonlinear effects can be tolerated will depend on the application. In the case of ILC, the phase space distortion introduced by a bunch compressor with the above parameters would lead to a significant loss of luminosity. We have to do something about it... but what?

If we inspect the phase space plots, then it seems that the damage is done by a second-order term in the map for the chicane, i.e. by a dependence of a change in z on the square of the energy deviation δ: such a term is a possible cause of the "parabolic" disortion that we see in the final phase space plot.

Assuming that our conjecture is correct, we could try to fix the distortion by modifying the map for the rf...

Consider a particle entering the bunch compressor with initial phase space co-ordinates z_0 and δ_0. We can write the co-ordinates z_1 and δ_1 of the particle after the rf cavity *to second order* in z_0 and δ_0:

$$z_1 = z_0, \tag{23}$$
$$\delta_1 = \delta_0 + R_{65}z_0 + T_{655}z_0^2. \tag{24}$$

Note that we have generalised the notation for the coefficients in the map: the first subscript indicates the variable on the left hand side of the equation, and subsequent subscripts indicate the variables in the relevant term. By convention, coefficients of linear terms are denoted R, coefficients of second-order terms are denoted T, third-order terms U and so on.

The coordinates of the particle after the chicane are then (again to second order):

$$z_2 = z_1 + R_{56}\delta_1 + T_{566}\delta_1^2, \tag{25}$$
$$\delta_2 = \delta_1. \tag{26}$$

If we combine the maps for the rf and the chicane, we get:

$$
\begin{aligned}
z_2 \;=\; & (1 + R_{56}R_{65})z_0 + R_{56}\delta_0 \\
& + (R_{56}T_{655} + R_{65}^2 T_{566})z_0^2 \\
& + 2R_{65}T_{566}z_0\delta_0 \\
& + T_{566}\delta_0^2,
\end{aligned}
\tag{27}
$$

$$
\delta_2 \;=\; \delta_0 + R_{65}z_0 + T_{655}z_0^2.
\tag{28}
$$

The term that gives the strong nonlinear distortion is the term in z_0^2 in (27). If we can design a system such that the appropriate coefficients satisfy:

$$
R_{56}T_{655} + R_{65}^2 T_{566} = 0,
\tag{29}
$$

then we should be able to reduce the distortion.

The values of $R_{56} = b$ and $R_{65} = -a$ are determined by the requirements for the compression factor. The value of T_{566} is determined by the chicane; in fact, we find for $\theta_0 \ll 1$ (see Exercise 1):

$$
T_{566} \approx -3L_1\theta_0^2 \approx -\frac{3}{2}R_{56}.
\tag{30}
$$

That leaves us with T_{655}. This is the second-order dependence of the energy deviation on longitudinal position for a particle passing through the rf cavity. But if we inspect the full rf map (3), we find it contains only odd-order terms, unless…

...we operate the rf cavity off-phase. In other words, if we modify the rf map to:

$$z \mapsto z, \tag{31}$$

$$\delta \mapsto \delta - \frac{eV}{E_0} \sin\left(\frac{\omega z}{c} + \phi_0\right). \tag{32}$$

The first-order coefficient in the map for δ is then:

$$R_{65} = -\frac{eV}{E_0}\frac{\omega}{c}\cos\phi_0. \tag{33}$$

The second-order coefficient is:

$$T_{655} = \frac{1}{2}\frac{eV}{E_0}\left(\frac{\omega}{c}\right)^2 \sin\phi_0. \tag{34}$$

Note that there is also a zeroth-order term, so the bunch ends up with a non-zero mean energy deviation $\langle\delta\rangle$ after the rf cavity; but we can take this into account simply by an appropriate scaling of the field in the chicane.

For the ILC bunch compressor, we now have the following coefficients. The linear coefficients are determined by the required compression factor, and the requirement to have no final correlation $\langle z\delta\rangle$:

$$R_{65} = -4.9937\,\text{m}^{-1}, \quad \text{and} \quad R_{56} = 0.19975\,\text{m}. \tag{35}$$

The value of T_{566} is determined by the R_{56} of the chicane:

$$T_{566} = -\frac{3}{2}R_{56} = -0.29963\,\text{m}. \tag{36}$$

And the value of T_{655} is determined by the desire to correct the second-order distortion of the phase space:

$$R_{56}T_{655} + R_{65}^2 T_{566} = 0 \quad \therefore \quad T_{655} = 37.406\,\text{m}^{-2}. \tag{37}$$

Now, given:

$$R_{65} = -\frac{eV}{E_0}\frac{\omega}{c}\cos\phi_0 = -4.9937\,\mathrm{m}^{-1}, \qquad (38)$$

and:

$$T_{655} = \frac{1}{2}\frac{eV}{E_0}\left(\frac{\omega}{c}\right)^2\sin\phi_0 = 37.406\,\mathrm{m}^{-2}, \qquad (39)$$

we find, for $E_0 = 5\,\mathrm{GeV}$ and $\omega = 1.3\,\mathrm{GHz}$:

$$V = 1,046\,\mathrm{MV}, \quad \text{and} \quad \phi_0 = 28.8°. \qquad (40)$$

Note that operating with this phase, we are providing over a gigavolt of rf to *decelerate* the beam by more than 500 MV. Because of adiabatic (anti)damping, we will need to reduce the R_{56} of the chicane by a factor E_1/E_0, where E_0 and E_1 are the mean bunch energy before and after the rf, respectively. Also, the phase space area occupied by the distribution will be increased by a factor E_0/E_1.

As usual, we illustrate the effect of the bunch compressor on phase space using a "window frame" distribution. Now we use the parameters determined above, to try to compress by a factor 20, while minimising the second-order distortion:
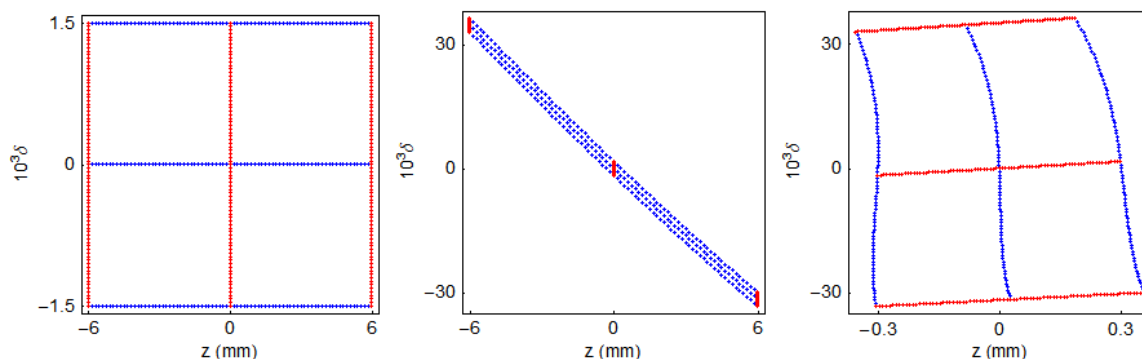
This looks much better: the dominant distortion now appears to be third-order, and looks small enough that it may not significantly affect the performance of the collider (though, of course, this would need to be checked by more detailed studies).

Bunch compressor: some conclusions

We have already learned some important lessons from this example:

- Ignoring nonlinear effects can get you into trouble. Sometimes you can get away with it; other times, a system designed without taking into account nonlinearities will not achieve the specified performance.

- If we take the trouble to analyse and understand the nonlinear behaviour of a system, then, if we are lucky and clever enough, we may be able to devise a means of compensating any adverse effects.

Second example: a simple storage ring

As a second example, let us consider the transverse dynamics in a simple storage ring. We shall assume that:

- The storage ring is constructed from some number of identical cells consisting of dipoles, quadrupoles and sextupoles.

- The phase advance per cell can be tuned from close to zero, up to about $0.5 \times 2\pi$.

- There is one sextupole per cell, which is located at a point where the horizontal beta function is $1\,\mathrm{m}$, and the alpha function is zero.

Usually, storage ring will contain two sextupoles per cell, to correct horizontal and vertical chromaticity. To keep things simple, we will use only one sextupole per cell.

The chromaticity, and hence the sextupole strength, will normally be a function of the phase advance. However, just to investigate the system, let us keep a fixed sextupole strength $k_2 L$, and see what happens as we adjust the phase advance.

We can assume that the map from one sextupole to the next is linear, and corresponds to a rotation in phase space through an angle given by the phase advance:

$$\begin{pmatrix} x \\ p_x \end{pmatrix} \mapsto \begin{pmatrix} \cos \mu_x & \sin \mu_x \\ -\sin \mu_x & \cos \mu_x \end{pmatrix} \cdot \begin{pmatrix} x \\ p_x \end{pmatrix}. \qquad (41)$$

Again to keep things simple, we shall consider only horizontal motion, and assume that the vertical coordinate $y = 0$ throughout.

The change in the horizontal momentum of a particle moving through the sextupole is found by integrating the Lorentz force:

$$\Delta p_x = -\int_0^L \frac{B_y}{B\rho}\, ds. \qquad (42)$$

The sextupole strength k_2 is defined by:

$$k_2 = \frac{1}{B\rho}\frac{\partial^2 B_y}{\partial x^2}, \qquad (43)$$

where $B\rho$ is the beam rigidity. For a pure sextupole field (assuming that the vertical coordinate $y = 0$),

$$\frac{B_y}{B\rho} = \frac{1}{2}k_2 x^2. \qquad (44)$$

If the sextupole is short, then we can neglect the small change in the coordinate x as the particle moves through the sextupole, in which case:

$$\Delta p_x \approx -\frac{1}{2}k_2 L x^2. \qquad (45)$$

The map for a particle moving through a short sextupole can be represented by a "kick" in the horizontal momentum:

$$x \;\mapsto\; x \tag{46}$$

$$p_x \;\mapsto\; p_x - \frac{1}{2}k_2 L x^2. \tag{47}$$

Let us choose a fixed value $k_2 L = -600\,\mathrm{m}^{-3}$, and see the effect of the maps for different phase advances. We examine the effect of the map in a given case by plotting the phase space coordinates after repeated action of the map (equation (41), followed by (46) and (47)) for a range of initial conditions. The resulting plot is known as a "phase space portrait".
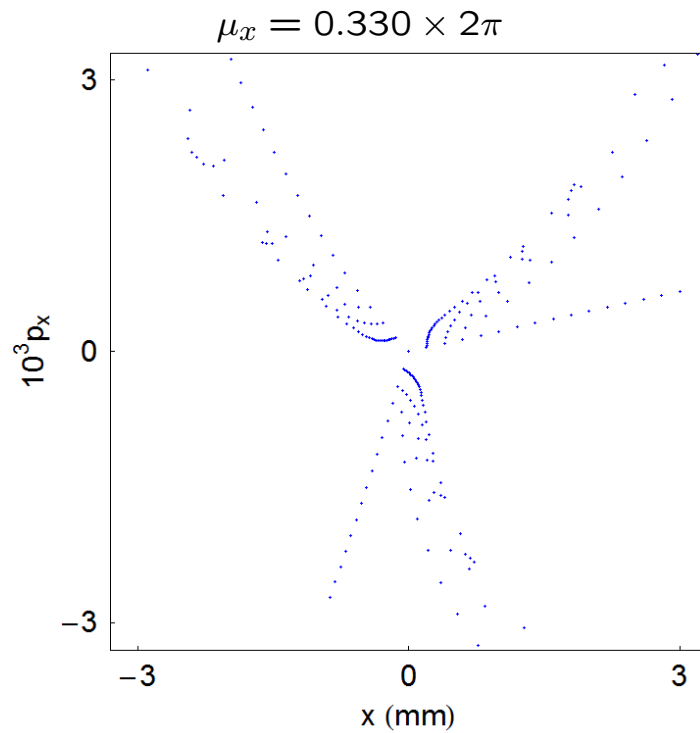
First, let us look at the phase space portraits for a range of phase advances from $0.2 \times 2\pi$ to $0.5 \times 2\pi$.
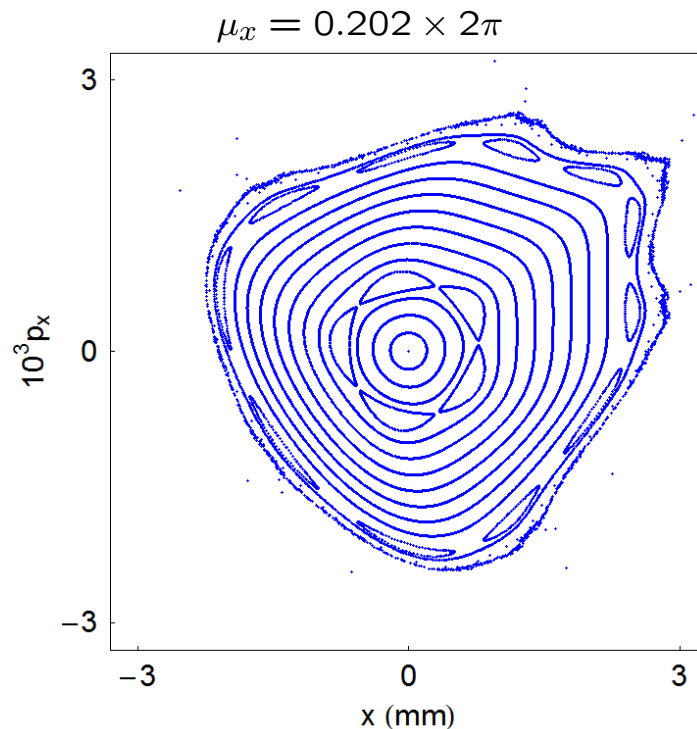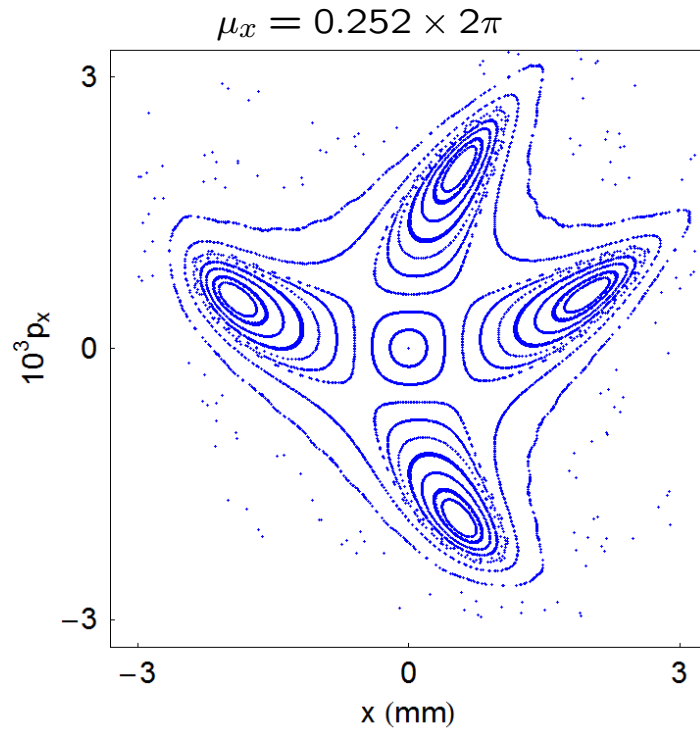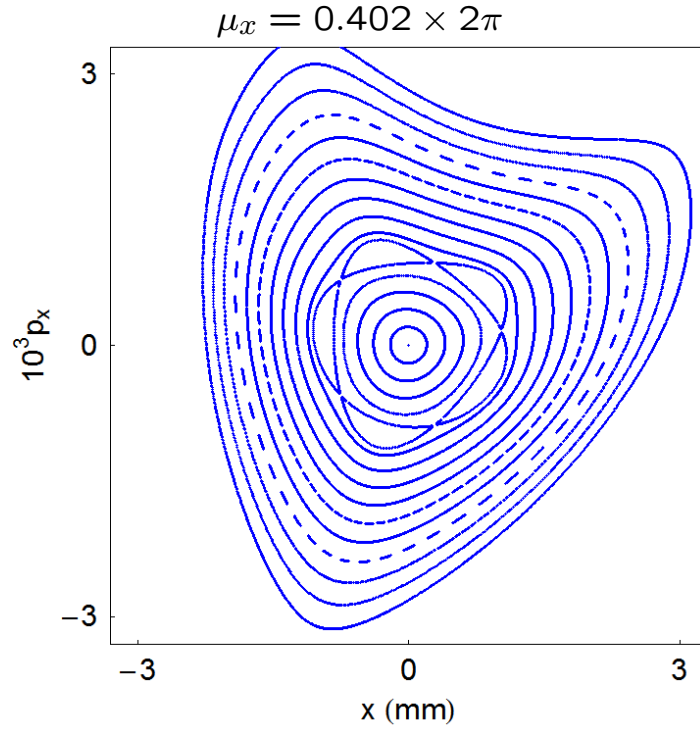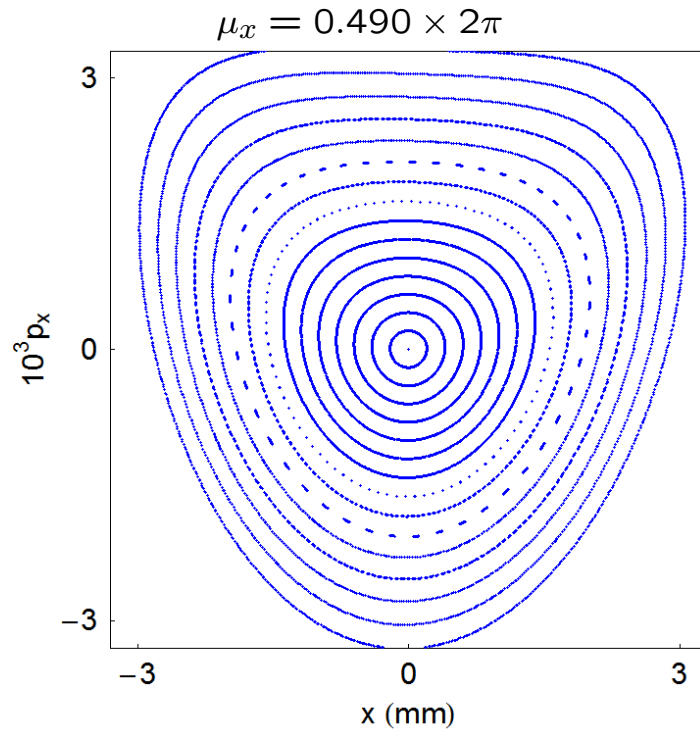
$$\mu_x = 0.202 \times 2\pi$$

Storage ring: nonlinear dynamics

$$\mu_x = 0.252 \times 2\pi$$

Storage ring: nonlinear dynamics

$$\mu_x = 0.330 \times 2\pi$$

Storage ring: nonlinear dynamics

$$\mu_x = 0.402 \times 2\pi$$

Storage ring: nonlinear dynamics

$$\mu_x = 0.490 \times 2\pi$$

Storage ring: nonlinear dynamics

There are some interesting features in these phase space portraits to which it is worth drawing attention:

- For small amplitudes (small x and p_x), particles map out closed loops around the origin: this is what we expect for a purely linear map.

- As the amplitude is increased, there appear "islands" in phase space: the phase advance (for the linear map) is generally close to one divided by the number of islands.

- Sometimes, a larger number of islands appears at larger amplitude.

- Usually, there is a closed curve that divides a region of stable motion from a region of unstable motion. Outside that curve, the amplitude of particles increases without limit as the map is repeatedly applied.

- The area of the stable region depends strongly on the phase advance: for a phase advance close to $2\pi/3$, it appears that the stable region almost vanishes altogether.

- It appears that as the phase advance is increased towards π, the stable area becomes large, and distortions from the linear ellipse become less evident.

Storage ring: nonlinear dynamics

We see already that the effect of the sextupole in the periodic cell depends strongly on the (linear) phase advance across the cell. In the (rather imprecise) language of beam dynamics, a phase advance of $2\pi m/n$, where m/n is an irreducible fraction, is said to be an "n^{th} order resonance".

Much of the rest of this course will be devoted to understanding in some detail the various phenomena that we have observed in this example, including resonances. However, we can understand at least some of the behaviour, by considering two special cases:

1. phase advance equal to an integer times 2π;

2. phase advance equal to a half integer times 2π.

Let us consider first what happens when the linear phase advance is an integer. In that case, the linear part of the map is just the identity:

$$x \;\mapsto\; x, \tag{48}$$

$$p_x \;\mapsto\; p_x. \tag{49}$$

So the combined effect of the linear map and the sextupole kick is:

$$x \;\mapsto\; x, \tag{50}$$

$$p_x \;\mapsto\; p_x - \frac{1}{2}k_2 L x^2. \tag{51}$$

Clearly, for $x \neq 0$, the horizontal momentum will increase without limit. There are no stable regions of phase space, apart from the line $x = 0$.

Now consider what happens if the phase advance is a half integer times 2π. In that case, the linear part of the map is a rotation through π. If a particle starts at the entrance of a sextupole with $x = x_0$ and $p_x = p_{x0}$, then at the exit of that sextupole, the phase space coordinates will be:

$$x_1 \;=\; x_0, \tag{52}$$

$$p_{x1} \;=\; p_{x0} - \frac{1}{2}k_2 L x_0^2. \tag{53}$$

Then, after passing to the entrance of the next sextupole, the coordinates will be:

$$x_2 \;=\; -x_1 = -x_0, \tag{54}$$

$$p_{x2} \;=\; -p_{x1} = -p_{x0} + \frac{1}{2}k_2 L x_0^2. \tag{55}$$

Now we go through the second sextupole (the one at which we have just arrived):

$$x_3 \;=\; x_2 = -x_0, \tag{56}$$

$$p_{x3} \;=\; p_{x2} - \frac{1}{2}k_2 L x_0^2 = -p_{x0}. \tag{57}$$

In other words, the momentum kicks from the two sextupoles cancel each other exactly. The resulting map is a purely linear phase space rotation by π. In this situation, we expect the motion to be stable (and periodic), no matter what the amplitude.

If we are designing a storage ring constructed of periodic cells with sextupoles, it appears to be beneficial for each cell to have a half-integer phase advance. But note that if there are two sextupoles per cell (as needed, for example, to correct vertical as well as horizontal chromaticity), the situation gets considerably more complicated. Also, there is another drawback. Consider what happens if, instead of the sextupole, we have a small focusing (quadrupole) error:

$$x \;\mapsto\; x, \tag{58}$$

$$p_x \;\mapsto\; p_x - k_1 L x. \tag{59}$$

It is a common technique in storage ring design to optimise the phase advance between sextupoles to give a good dynamic aperture, while using a non-periodic section of the lattice to control the overall tunes.

Third example: a final focus system

Finally, let us consider a final focus system in a collider. Such a system is designed to make the transverse beam size as small as possible, by focusing the beta functions to very small values at the interaction point. In its simplest form, a final focus system can consist of just a sequence of quadrupoles and drifts, i.e. just simple linear elements.

As a specific example, let us take a final focus system designed to reduce the beta functions from 10 m in each plane, to 5 mm in the horizontal, and 0.35 mm in the vertical.

We can use a standard beam dynamics code to design and model our final focus system. MAD8 is suitable for the job…
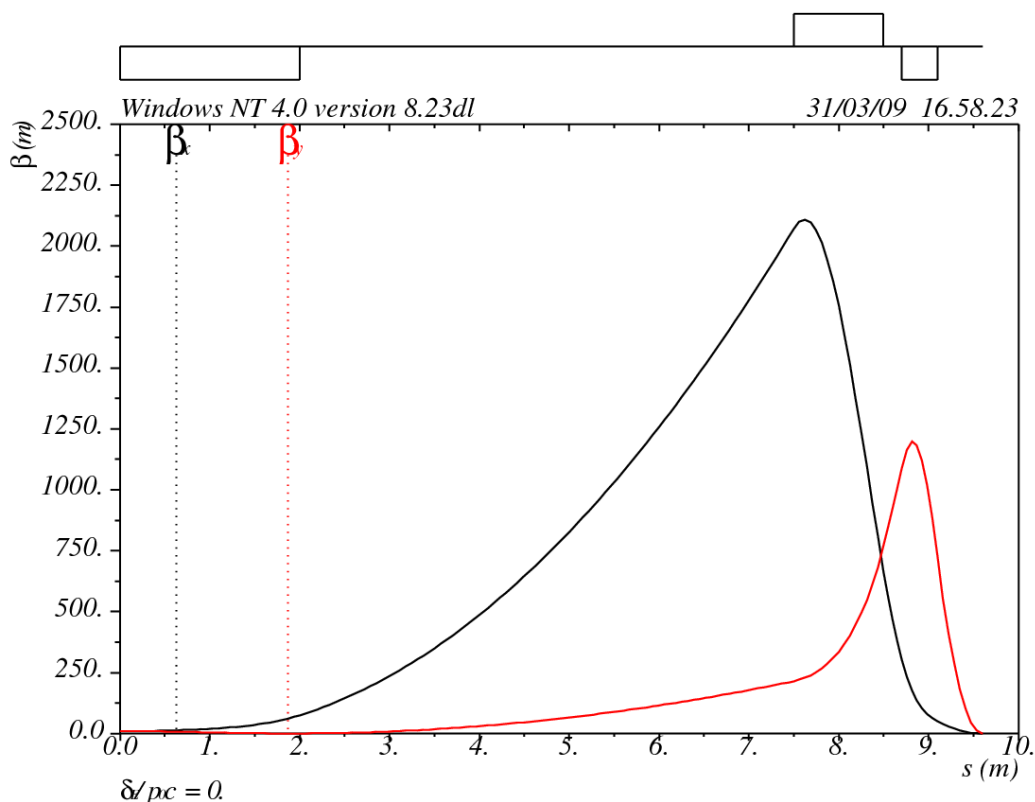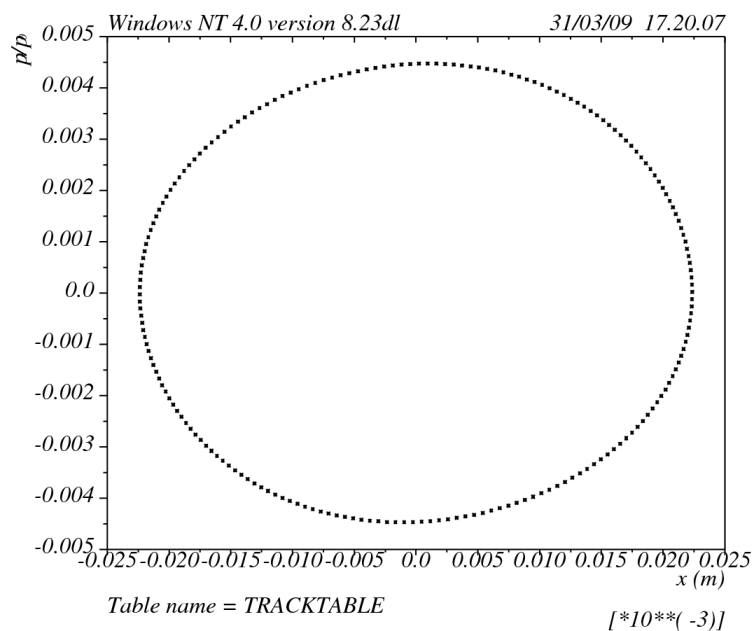
Final focus: linear dynamics

Let us track a phase space ellipse in the horizontal plane through the final focus. We shall use an initial ellipse corresponding to an rms beam size with emittance 100 nm, i.e. with a beta function of 10 m, the beam size is 1 mm.


Windows NT 4.0 version 8.23dl   *31/03/09 17.20.07*

Table name = TRACKTABLE

[*10**(-3)]
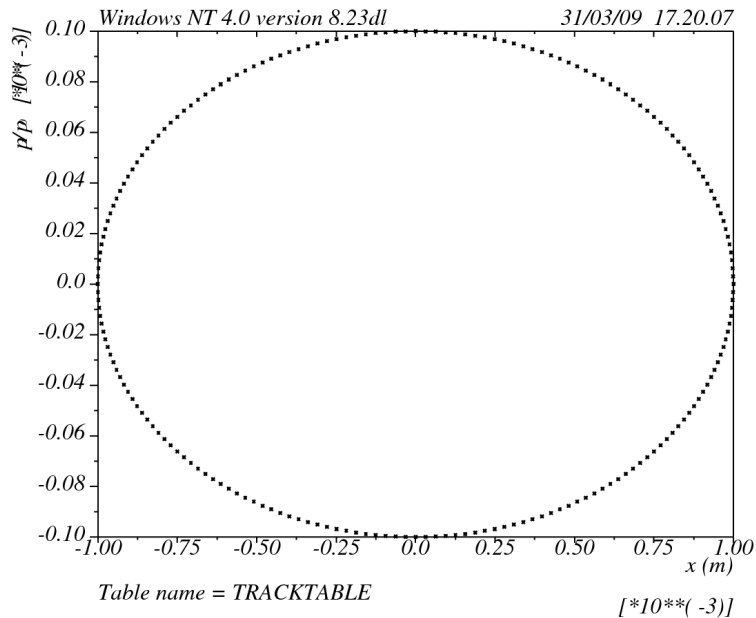
Final focus: linear dynamics

Tracking the ellipse to the interaction point, we obtain, as expected, an ellipse corresponding to reduced beam size (22 μm), and increased divergence.

Windows NT 4.0 version 8.23dl   *31/03/09 17.20.07*

Table name = TRACKTABLE

[*10**(-3)]

Final focus: linear dynamics

So far so good. But what happens if we get more ambitious, and try to squeeze the beta functions at the interaction point, to 1 mm horizontally, and 0.25 mm vertically? First of all, the beta functions through the system peak at larger values.
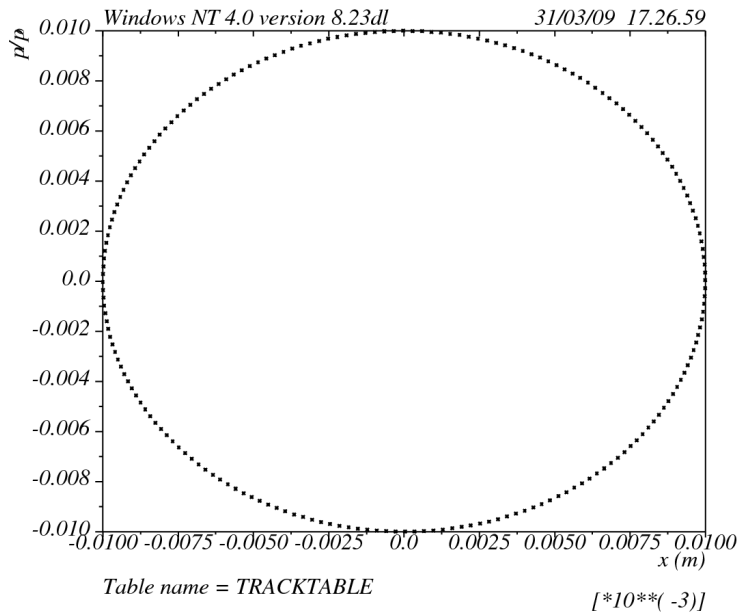
Final focus: nonlinear dynamics
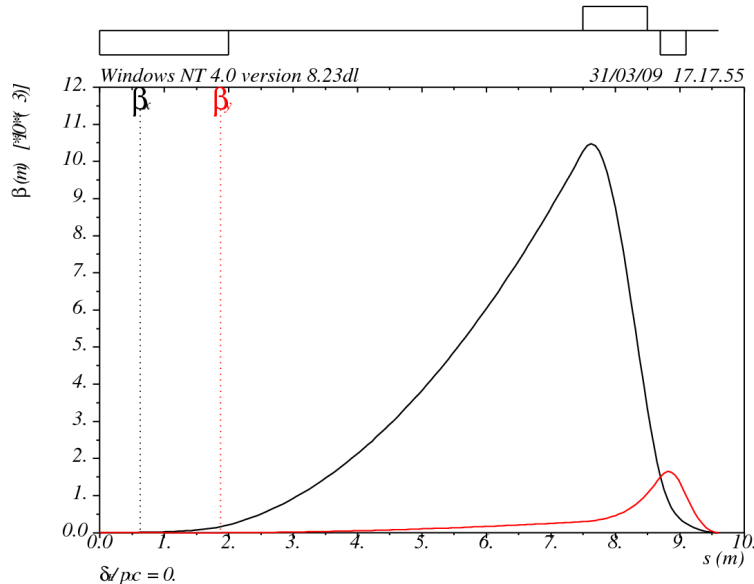
More worryingly, when we track the same phase space ellipse as before, we now obtain a distribution at the interaction point that shows significant distortion (despite the fact that the beamline contains only "linear" elements).
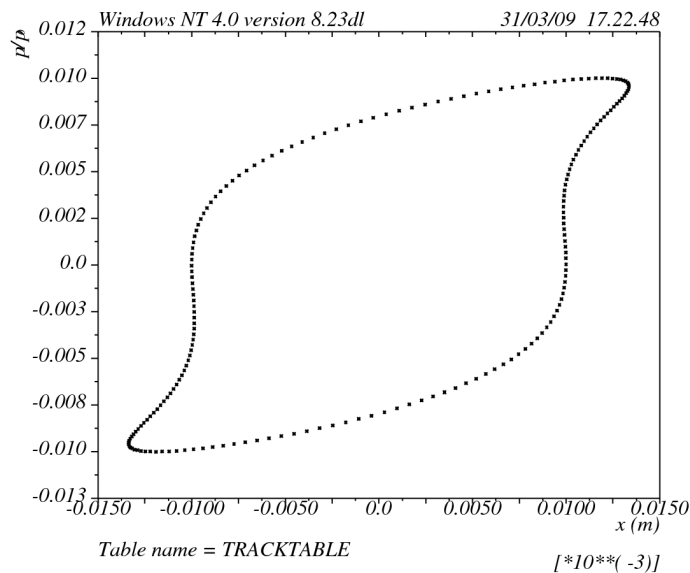
Note: we obtain this result using the LIE4 tracking algorithm in MAD8.

More disturbing still, when we try alternative tracking algorithms in MAD8 (LIE3, or TRANSPORT), the distortion disappears, and we obtain the regular ellipse corresponding to linear motion.

Windows NT 4.0 version 8.23dl   31/03/09 17.26.59

Table name = TRACKTABLE

[*10**(-3)]

Final focus: nonlinear dynamics

If the real system behaves as predicted by LIE4, we would be in trouble. However, we need to ask some questions:

- Is the nonlinear distortion we observe with LIE4 tracking real? If so, where does it come from?

- Why does the tracking with LIE4 look different from LIE3 and TRANSPORT?

- If the nonlinear distortion is real, what can we do about it?

These are questions that we shall attempt to answer as we work through this course...

Summary

- Nonlinear effects are important in many diverse accelerator systems, and can arise even in systems comprising elements that are often considered "linear".

- Nonlinear effects can occur in the longitudinal or transverse motion of particles moving along an accelerator beam line.

- To understand nonlinear dynamics in accelerators we need to be able to (1) construct dynamical maps for individual elements and complete systems, and (2) analyse these maps to understand the impact of nonlinearities on the performance of the system.

- If we have an accurate and thorough understanding of nonlinear dynamics in accelerators, then we can attempt to mitigate any adverse effects from nonlinearities.

Exercises

1. Show equation (30): for a chicane constructed from four dipoles, $T_{566} = -\frac{3}{2}R_{56}$.

2. Using Matlab, Scilab, or some other scientific software, write a program to construct the phase space portraits shown in slides $33 - 37$. How are the phase space portraits changed if the beta function is different from unity? Make a plot of the largest stable orbit amplitude as a function of linear phase advance.

3. Consider a storage ring constructed from repeated unit cells, with a transverse phase advance of π across each cell. If there is a small focusing error k_1L at the same location in each cell, where the beta function is 1 m, write down the phase space coordinates after passing through N cells, starting (immediately after one focusing error) with $x = x_0$ and $p_x = 0$.

4. Look up the MAD8 Physical Methods Manual. Use the information in this manual to explain the nonlinearities observed in the final focus system described above, and why they are observed only when the LIE4 tracking algorithm is used.